High-resolution neutron-scattering study of slow dynamics of surface water molecules in zirconium oxide

E. Mamontov[a)]

National Institute of Standards and Technology (NIST) Center for Neutron Research, National Institute of Standards and Technology, Gaithersburg, Maryland 20899-8562 and Department of Materials Science and Engineering, University of Maryland, College Park, Maryland 20742-2115

(Received 18 March 2005; accepted 16 May 2005; published online 19 July 2005)

We have performed a quasielastic neutron-scattering experiment on backscattering spectrometer with sub-μeV resolution to investigate the slow dynamics of surface water in zirconium oxide using the sample studied previously with a time-of-flight neutron spectrometer [E. Mamontov, J. Chem. Phys. **121**, 9087 (2004)]. The backscattering measurements in the temperature range of 240–300 K have revealed a translational dynamics slower by another order of magnitude compared to the translational dynamics of the outer hydration layer observed in the time-of-flight experiment. The relaxation function of this slow motion is described by a stretched exponential with the stretch factors between 0.8 and 0.9, indicating a distribution of the relaxation times. The temperature dependence of the average residence time is non-Arrhenius, suggesting that the translational motion studied in this work is more complex than surface jump diffusion previously observed for the molecules of the outer hydration layer. The observed slow dynamics is ascribed to the molecules of the inner hydration layer that form more hydrogen bonds compared to the molecules of the outer hydration layer. Despite being slower by two orders of magnitude, the translational motion of the molecules of the inner hydration layer may have more in common with bulk water compared to the outer hydration layer, the dynamics of which is slower than that of bulk water by just one order of magnitude. © *2005 American Institute of Physics*. [DOI: 10.1063/1.1949171]

I. INTRODUCTION

Quasielastic neutron scattering (QENS) has been frequently used to study the influence of the level of hydration on the mobility of confined and interface water in various inorganic (Vycor glass,[1] zeolite,[2] and cement pastes[3]) and organic (purple membrane,[4] C-phycocyanin,[5] and *N*-acetyl-leucine-methylamide[6]) materials. In general, the water diffusivity increases with the increasing hydration. While the hydration level dependence of water mobility is of considerable importance in technology, its most profound implication may be in the area of life science. For example, recent experimental observations[6] seem to affirm the previously suggested hypothesis that limited dynamics of surface water below a certain critical hydration level preclude proteins function. Therefore, understanding the interaction of water molecules with each other and with the surface as a function of hydration level is of significant interest.

Intuitively, in the presence of more than one hydration layer, the dynamics of the inner layer should be affected by the interaction with the surface to the largest extent, whereas the dynamics of the outer layers should be more bulklike. However, in the case of surface water the dynamics of the outermost hydration layer may differ qualitatively from that of bulk water owing to a lower number of hydrogen bonds that the water molecules form with the nearest neighbors.[7] On the other hand, the environment for the water molecules between the surface and the outermost hydration layer may bear more similarity to that in bulk water. Thus, the dynamics of such water molecules, even though greatly affected by the interaction with the surface, may be expected to exhibit some features of bulk water dynamics unseen in the outermost hydration layer.

In a recent paper,[7] we described the dynamics of surface water in ZrO_2 in the temperature range of 300–360 K measured by quasielastic neutron scattering using a cold time-of-flight neutron spectrometer operated with an energy resolution of 19 μeV (full width at half maximum). The high surface area powder zirconium oxide sample had about two layers of molecular water on top of the surface hydroxyl groups. We concluded that the dynamics accessible in the measurements with a 19-μeV resolution was associated with the water molecules of the outer hydration layer. The characteristic times associated with the dynamics of these molecules were in the range of tens of picoseconds.

In this work, we studied the same ZrO_2 sample in the temperature range of 240–300 K using a backscattering neutron spectrometer. A very high resolution of the spectrometer (less than 1 μeV, full width at half maximum) provided an insight into the much slower dynamics of water molecules. The translational dynamics that we observed was characterized by the relaxation times in the range of 500–1000 ps. We ascribed the observed dynamics to the motion of water molecules of the inner hydration layer. Despite showing the translational dynamics slower by an order of magnitude compared to the outer hydration layer, the inner hydration layer bears more resemblance to bulk water compared to the

a)FAX: (301) 921-9847. Electronic mail: mamontov@nist.gov

outer hydration layer. The dynamics of the inner hydration layer could be described by a relaxation function in the form of a stretched exponential, indicating a distribution of the relaxation times. Another similarity to bulk water was indicated by a deviation of the temperature dependence of the average residence time from Arrhenius-type behavior. Non-Arrhenius behavior indicated that, unlike the water molecules of the outer hydration layer, the molecules of the inner hydration layer form more hydrogen bonds. Similar to bulk water, and in contrast with the outer hydration layer, a translational diffusion process for the molecules of the inner hydration layer may involve a rearrangement of the neighboring molecules resulting in a nonexponential relaxation function and non-Arrhenius temperature dependence of the relaxation time. We propose that in the absence of the outer hydration layer, the water layer in contact with the surface hydroxyl groups would demonstrate the translational dynamics with an Arrhenius-type temperature dependence and a characteristic residence time of tens of picoseconds, similar to what we have observed for the outer hydration layer. It is the presence of the outer hydration layer that slows down the dynamics of the inner hydration layer from tens to hundreds of picoseconds.

II. EXPERIMENT

The characterization and pretreatment of the high surface area ZrO_2 powder sample obtained from Magnesium Elektron Inc., New Jersey, have been described elsewhere.[7] In brief, the sample with a surface area of 80 m^2/g had about two layers of molecular water on top of the surface hydroxyl groups. Water-containing zirconium oxide powder was placed in a thin annular aluminum sample holder chosen to ensure greater than 90% neutron beam transmission through the sample. The sample was sealed with an indium O ring, and mounted onto the cold stage of a closed-cycle refrigerator, the temperature of which was controlled within ± 0.1 K. QENS experiment was performed using the high-flux backscattering spectrometer[8] (HFBS) at the National Institute of Standards and Technology (NIST) Center for Neutron Research. The incident neutron wavelength at the HFBS is varied via Doppler shifting about a nominal value of 6.271 Å ($E_0=2.08$ meV). After scattering from the sample, only neutrons having a fixed final energy of 2.08 meV are measured by the detectors as ensured by Bragg reflection from analyzer crystals. The instrument was operated with a dynamic range of ± 11 μeV to provide the best energy resolution and the highest neutron counting rates. With this dynamic range, the full width of the sample-dependent instrument resolution function at half maximum was 0.85 μeV, as measured with the sample cooled down to 5 K.

The data collected at seven detectors ($0.75\ \text{Å}^{-1} < Q < 1.42\ \text{Å}^{-1}$ at the elastic channel) have been used in the data analysis. Following the collection of QENS spectra at 300, 280, 260, and 240 K, the data were collected at 5 K to obtain the sample-dependent instrument resolution function. Then the indium seal was removed, and the sample was evacuated *in situ* for 30 min at $T=290$ K to about 10^{-5} torr using a turbopump. The final set of data collected from the evacuated sample demonstrated that even a short evacuation at room temperature eliminates virtually all quasielastic signal. This observation reassures us that the QENS signal collected at the backscattering spectrometer originates from easily removable surface water rather than water confined in closed pores.

III. RESULTS AND ANALYSIS

As in the earlier paper,[7] only a limited Q range could be used for data analysis. The data in the high-Q region had to be discarded because of the strong Bragg scattering from zirconia. On the other hand, the scattering from the first Bragg peak of monoclinic ZrO_2, a very weak (100) peak at $Q=1.23\ \text{Å}^{-1}$, did not deem the data collected around this Q point unusable. In the low-Q region, the signal was dominated by the elastic small-angle scattering from small zirconia particles. Compared to the previous work,[7] where the low-Q data region could not be used because of the small-angle scattering, the choice of the low-Q limit for the analysis of the slow water dynamics is even more restricted because of the presence of the fast (on the time scale of the backscattering spectrometer) water that we have studied previously using a time-of-flight spectrometer. The presence of the "fast" water is insignificant for the analysis of the dynamics of the "slow" water at high Q because quasielastic scattering from the fast water becomes too broad for the backscattering spectrometer dynamic range and appears as almost flat background in the data. For translational jump diffusion, the quasielastic broadening at sufficiently high Q approaches the value of $\hbar/\tau$, where τ is the residence time, and is much wider for the fast water with its short residence time. At the low Q, however, the broadening follows the $\hbar DQ^2$ dependence, where D is the diffusion coefficient, and the width of the quasielastic scattering from fast water may be sufficiently small to contribute to the quasielastic signal detectable in the dynamic range of the backscattering spectrometer. Our choice of the Q range for the data analysis ($0.75\ \text{Å}^{-1} < Q < 1.42\ \text{Å}^{-1}$ at the elastic channel) was made in order to ensure that the quasielastic signal we analyzed was due to slow water, since at lower Q a broad quasielastic scattering component due to fast water was still detectable. Indeed, based on the values of the residence time and diffusion jump distance previously obtained for the fast water at 300 K,[7] we can expect the half width at half maximum (HWHM) for the corresponding QENS signal to be 4.6, 8.6, 12.7, and 15.7 μeV at $Q=0.25$, 0.36, 0.47, and 0.56 Å^{-1}, respectively, which are the Q values for the lowest-Q detectors of the HFBS. As we will demonstrate below, the residence time for the slow water is longer by an order of magnitude compared to that of fast water. Assuming a similar diffusion jump distance (which is expected to be at least not larger for the slow water than for the fast water), one can estimate the HWHM of the QENS signal from the slow water to be 0.5, 0.9, 1.3, and 1.6 μeV at $Q=0.25$, 0.36, 0.47, and 0.56 Å^{-1}, respectively. Because the four lowest-Q detectors of the HFBS are located in somewhat off backscattering positions, they have worsened energy resolution compared to the rest of the detectors.[8] Therefore, at low Q the QENS signal from the

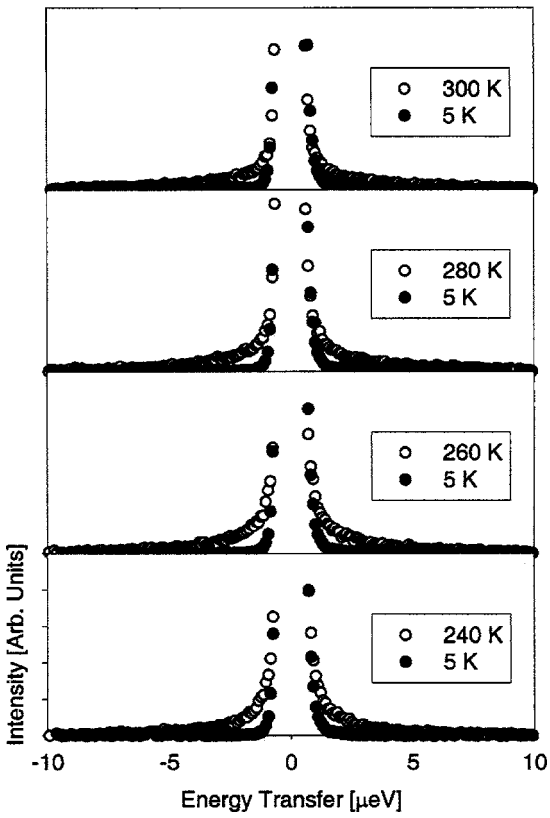

FIG. 1. The scattering intensities measured in the energy space at $Q = 1.11$ Å^{-1}. The linear background obtained from fitting the data using Eq. (1) is subtracted, and the elastic peaks at zero energy transfer are truncated to better demonstrate the quasielastic signal. The 5-K data used as a resolution function are plotted on every graph and shown with filled circles.

slow water is difficult to resolve, and all the detectable broadening originates from the fast water. This is even more certain for the lower temperatures of 280, 260, and 240 K, where all QENS signals become narrower.

It should be emphasized that omitting the low-Q portion of the data precludes reliable determination of the diffusion coefficient (or the diffusion jump length), but does not compromise the accuracy of the determination of the residence time, which depends on the high-Q data.

The data collected at $Q = 1.11$ Å^{-1} are shown in Fig. 1 as an example. The width of the quasielastic signal grows as the temperature is increased, indicating faster diffusion at higher temperatures. However, even at the highest temperature of 300 K the width of the signal is much smaller compared to the dynamic range of the measurements. In addition to the quasielastic signal from mobile water molecules, the spectra include a strong elastic line mainly due to the surface hydroxyl groups, and, possibly, water molecules which are immobile on the time scale of the experiment.

As a first step in the data analysis, we fit the data using the following expression with a simple Lorentzian quasielastic broadening:

$$I(Q,E) = C(Q)\left[x(Q)\,\delta(E) + [1 - x(Q)]\frac{1}{\pi}\frac{\Gamma(Q)}{E^2 + \Gamma^2(Q)}\right] + B_1E + B_2, \quad (1)$$

which was convolved with the spectrometer resolution function. Here C is a scaling constant, x is the fraction of the elastic scattering, and the linear term $B_1E + B_2$ describes the background due to inelastic scattering and possibly quasielastic scattering which is too broad for the dynamic range of the backscattering spectrometer. The Q dependence of the Lorentzian half-width at half maximum is plotted in Fig. 2. Except for the highest temperature, where significant scattering of the data points makes it difficult to see the trend, the width of the quasielastic broadening increases with Q, which is indicative of the translational jump diffusion with a distribution of jump length. Thus, we fit $\Gamma(Q)$ with the expression that was derived by Hall and Ross[9] for translational diffusion with a Gaussian distribution of jump length

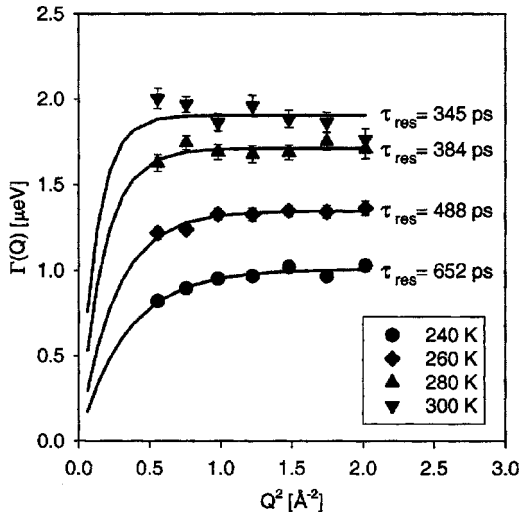

FIG. 2. Q dependence of the HWHM of the Lorentzian in Eq. (1) and its fitting using Eq. (2).

$$\Gamma(Q) = \frac{\hbar}{\tau_{\text{res}}}[1 - \exp(-Q^2\langle r^2\rangle/6)], \quad (2)$$

where $\langle r^2\rangle$ is a mean-square jump length, and τ_{res} is a residence time between jumps. In the earlier analysis of the dynamics of the fast water based on the time-of-flight data collected with the dynamic range of $\pm$ 500 μeV, the expressions more complex than a single Lorentzian had to be used for the quasielastic broadening in order to take into consideration both the translational and rotational components of the water diffusion.[7,10] This was necessary because the characteristic relaxation times for the two components differed by an order of magnitude, and both components contributed to the quasielastic signal detectable within the dynamic range of the measurement. Since the rotational component tends to be affected by the confinement to a smaller extent compared to the translational component, the separation of the time scales between the two components can be expected only to grow as the dynamics of the confined water slows down. Along with the narrow dynamic range of the measurement of $\pm$11 μeV, this suggests that Eqs. (1) and (2) or an alternative formalism that takes into account only the translational diffusion component can be successfully used for the analysis of our data obtained with the backscattering spectrometer. We also have tried to use an expression similar to Eq. (1) that includes two Lorentzians with similar weights and variable

$\Gamma(Q)$ to investigate a possible presence of a broad component due to the fast water in the data. We found that no distinct broad component, the width of which would decrease with the decreasing temperature, could be detected, perhaps because of a relatively high background of the spectrometer and a limited dynamic range of the measurement.

As the next step in the data analysis, the scattering intensities including the resolution function (the data collected 5 K) were Fourier-transformed into the time space following the subtraction of a linear background term, B_1E+B_2, obtained from fitting using Eq. (1) and the correction for a small zero energy offset. The Fourier transformation could be applied to the data without introducing a significant termination error, thanks to a small width of the narrow quasielastic signal that decays to zero at the extremes of the dynamic range. Without subtraction of the linear background, however, the data distortion in the time space would be pronounced at the short times. Since convolution with the resolution function in the energy space is replaced by a simple multiplication in the time space, the resulting scattering intensities in the time space were then divided by the Fourier-transformed resolution function yielding intermediate scattering functions $I(Q,t)$ that we fitted with the expression analogous to Eq. (1):

$$I(Q,t) = C(Q)\left\{x(Q) + [1 - x(Q)]A(Q)\exp\left[-\left(\frac{t}{\tau}\right)^{\beta}\right]\right\}, \tag{3}$$

where $A(Q)$ is the elastic incoherent structure factor (EISF). When $A(Q)=1$ and $\beta=1$, Eq. (3) is obtained by a Fourier transformation of Eq. (1). The exponential term, $\exp(-t/\tau)$ in the relaxation function is a Fourier transformation of the Lorentzian with the HWHM equal to the relaxation rate, $\Gamma(Q)=(\hbar/\tau)$. A stretched exponential relaxation function with $0<\beta<1$ has been used to describe the dynamics of supercooled water[1,11] and water in confinement.[12,13] The formalism that uses a stretched exponential for a relaxation function was originally developed as a result of applying the mode coupling theory (MCT) to a supercooled water.[1,11] It was proposed that, for the time intervals longer than 1 ps, $A(Q)$ should be equal to $\exp(-Q^2a^2/3)$, where a describes the root-mean-square vibrational amplitude of a water molecule in the "cage" formed by the neighboring water molecules, in which the water molecule is constrained during its short-time movements, or simply the radius of such a cage. In our analysis, the parameter $A(Q)$ was coupled to the fraction of elastic scattering, $x(Q)$, which was a variable parameter. Only if the elastic signal could be subtracted from the data it would be possible to extract the functional dependence of $A(Q)$ from the Q dependence of the scattering intensity.

It should be noted that an approach alternative to the MCT theory that uses a glasslike model of water with a distribution of correlation times[12] also yields the functional dependence for the relaxation function in the form of a stretched exponential. The glassy state model is thought to be applicable for a deeper supercooled regime.[12] Even though the underlying principles and the ranges of applicability for the mode coupling theory and glassy state model are different, the relaxation function in the form of a stretched exponential is similar in both models.

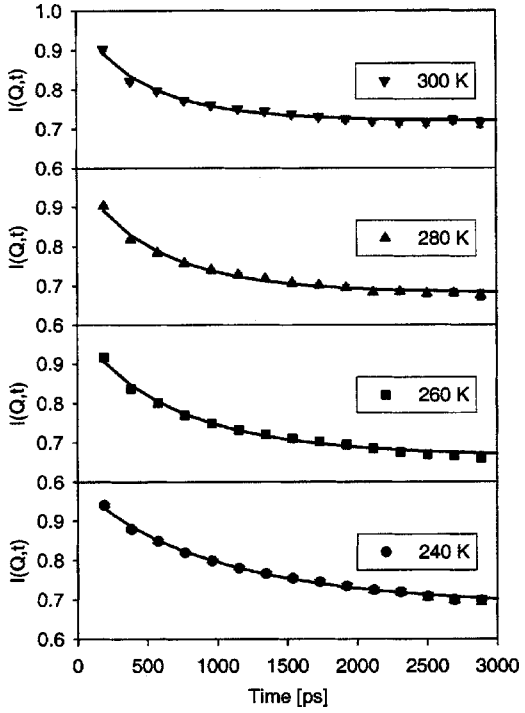

FIG. 3. The intermediate scattering functions $I(Q,t)$ obtained from Fourier transformation of the scattering intensities collected at $Q=1.11$ Å^{-1} and their fitting using the relaxation function in the form of a stretched exponential [Eq. (3)].

An example of the fit in the time space using Eq. (3) for the data measured at $Q=1.11$ Å^{-1} is shown in Fig. 3. Note that at the long time the intermediate scattering functions decay not to zero, but to the constant background values determined by the fraction of the elastic scattering [see Eq. (3)]. As the temperature is decreased, the decay of the relaxation function to the background is observed over longer-time periods, indicating slower dynamics of mobile water molecules. The values of τ and β are summarized in Table I along with the corresponding standard deviations. At each temperature, a remarkably low scattering in the β values through the Q range suggests that a universal Q-independent value of the stretch factor can be used for the data fitting. Such averaged values calculated as $\langle\beta\rangle=\Sigma(\beta_i/\sigma_i^2)/\Sigma(1/\sigma_i^2)$ are also listed in Table I along with the corresponding $\langle\tau\rangle_\beta$ obtained using Eq. (3) with fixed Q-averaged stretch factors $\langle\beta\rangle$. The difference between the corresponding values of τ and $\langle\tau\rangle_\beta$ is small, while the standard deviations for the $\langle\tau\rangle_\beta$ are significantly lower.

The Q dependence of the inverse relaxation time, $1/\langle\tau\rangle_\beta$, is plotted in Fig. 4. As one can see by comparing Figs. 4 and 2, a similar Q dependence was demonstrated by the Lorentzian HWHM, $\Gamma(Q)$. Therefore, we fit the relaxation rate with an expression similar to Eq. (2), $(\hbar/\langle\tau_0\rangle_\beta)(1-\exp\times(-Q^2\langle r^2\rangle/6))$, and obtain the values for the parameter $\langle\tau_0\rangle_\beta$, as listed in Table I. Unlike τ_{res} in Eq. (2), the parameter $\langle\tau_0\rangle_\beta$ does not represent the residence time, but merely describes the Q dependence of the relaxation rate (inverse re-

TABLE I. Parameters β and τ obtained from fitting the data in the time space using Eq. (3). Standard deviation values are shown in parentheses. Also shown are Q-averaged stretch factors, $\langle\beta\rangle$, parameters $\langle\tau\rangle_\beta$ obtained using fixed values of $\langle\beta\rangle$ in Eq. (3), and parameters $\langle\tau_0\rangle_\beta$ obtained from fitting the Q dependence of $\langle\tau\rangle_\beta$ with the expression $(\hbar/\langle\tau_0\rangle_\beta)(1-\exp(-Q^2\langle r^2\rangle/6))$.

	$T=240$ K			$T=260$ K			$T=280$ K			$T=300$ K		
	$\langle\tau_0\rangle_\beta=976(17)$ ps $\langle\beta\rangle=0.84(0.02)$			$\langle\tau_0\rangle_\beta=666(10)$ ps $\langle\beta\rangle=0.86(0.01)$			$\langle\tau_0\rangle_\beta=531(7)$ ps $\langle\beta\rangle=0.85(0.01)$			$\langle\tau_0\rangle_\beta=460(13)$ ps $\langle\beta\rangle=0.85(0.01)$		
Q (Å^{-1})	β	τ(ps)	$\langle\tau\rangle_\beta$(ps)	β	τ(ps)	$\langle\tau\rangle_\beta$(ps)	β	τ(ps)	$\langle\tau\rangle_\beta$(ps)	β	τ(ps)	$\langle\tau\rangle_\beta$(ps)
0.75	0.80	1259	1158	0.82	786	749	0.85	538	537	0.82	440	435
	(0.05)	(193)	(68)	(0.04)	(53)	(28)	(0.04)	(23)	(19)	(0.04)	(18)	(15)
0.87	0.86	1040	1083	0.88	711	722	0.84	518	516	0.89	426	433
	(0.05)	(106)	(59)	(0.04)	(39)	(28)	(0.04)	(22)	(18)	(0.04)	(15)	(15)
0.99	0.84	1027	1036	0.89	628	646	0.84	537	533	0.87	457	462
	(0.04)	(90)	(45)	(0.03)	(24)	(19)	(0.03)	(21)	(16)	(0.04)	(17)	(15)
1.11	0.88	974	1047	0.89	672	692	0.88	524	537	0.88	439	446
	(0.04)	(83)	(53)	(0.04)	(32)	(25)	(0.04)	(23)	(20)	(0.05)	(18)	(17)
1.22	0.85	936	949	0.88	650	663	0.85	545	543	0.81	507	491
	(0.03)	(67)	(36)	(0.03)	(27)	(20)	(0.03)	(22)	(17)	(0.03)	(23)	(16)
1.32	0.87	911	960	0.85	677	667	0.83	513	507	0.87	441	445
	(0.04)	(66)	(42)	(0.04)	(35)	(23)	(0.04)	(23)	(18)	(0.05)	(17)	(17)
1.42	0.81	1049	987	0.83	696	673	0.78	586	551	0.79	547	522
	(0.04)	(110)	(45)	(0.04)	(41)	(24)	(0.04)	(36)	(21)	(0.05)	(34)	(22)

laxation time), $1/\langle\tau\rangle_\beta$. The average relaxation time, which takes both parameters $\langle\beta\rangle$ and $\langle\tau\rangle_\beta$ into consideration, can be calculated as[1]

$$\langle\langle\tau\rangle_\beta\rangle = \int_0^\infty \exp\left[-\left(\frac{t}{\langle\tau\rangle_\beta}\right)^{\langle\beta\rangle}\right]dt = \frac{\langle\tau\rangle_\beta}{\langle\beta\rangle}\Gamma\left(\frac{1}{\langle\beta\rangle}\right), \tag{4}$$

where Γ is the gamma function. Figure 5 shows the inverse average relaxation time in the energy units, $\Delta E=\hbar/\langle\langle\tau\rangle_\beta\rangle$, as a function of Q^2. Fitting the inverse average relaxation time with

$$\Delta E = \frac{\hbar}{\langle\langle\tau\rangle_\beta\rangle} = \frac{\hbar}{\langle\tau_{\mathrm{res}}\rangle}[1-\exp(-Q^2\langle r^2\rangle/6)] \tag{5}$$

yields the average residence time, $\langle\tau_{\mathrm{res}}\rangle$ for the jump diffusion process with distributions of both the jump lengths and the residence times. Previously, Swenson *et al.*[13] have used similar expression to fit the Q dependence of the inverse average relaxation time for a slow component of interlayer water in a fully hydrated Na-vermiculite clay. Average residence times obtained from fitting with Eq. (5) are summarized in Table II.

Finally, we have to consider possible influence of the quasi-two-dimensional character of the translational motion of surface water on the parameters we obtain from the fitting. The effect of the two dimensionality can be evaluated if the functional Q dependence of the parameter τ is known. As we discussed before, the inverse relaxation time could be fitted with the expression $(\hbar/\tau_0)(1-\exp(-Q^2\langle r^2\rangle/6))$ (for the sake of simplicity, we now omit the notation $\langle\tau_0\rangle_\beta$ that indicates the averaging over β), which is the functional dependence for three-dimensional translational diffusion with a distribution of jump length. This means that in the three-dimensional

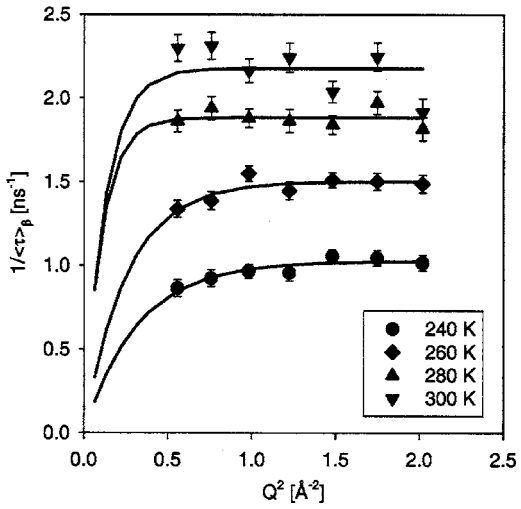

FIG. 4. Q dependence of the relaxation rate, $1/\langle\tau\rangle_\beta$, and its fitting with the expression $(\hbar/\langle\tau_0\rangle_\beta)(1-\exp(-Q^2\langle r^2\rangle/6))$.

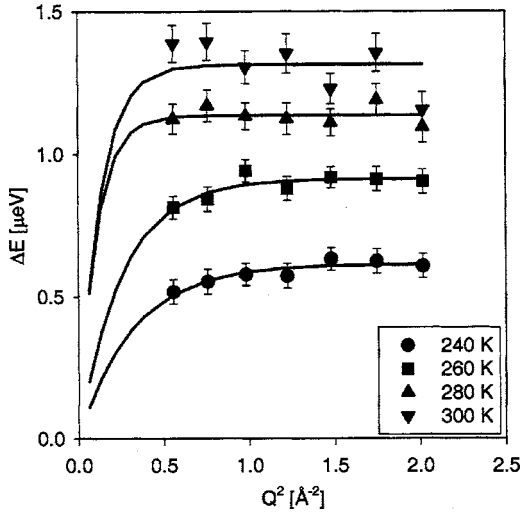

FIG. 5. Q dependence of the inverse average relaxation time in the energy units, $\Delta E=\hbar/\langle\langle\tau\rangle_\beta\rangle$, and its fitting using Eq. (5).

TABLE II. Average residence time obtained from fitting the inverse average relaxation time in the energy units, $\Delta E=\hbar/\langle\langle\tau\rangle_\beta\rangle$, with Eq. (5). Standard deviation values are shown in parentheses.

$T(K)$	$\langle\tau_{res}\rangle$(ps)
300	500 (16)
280	578 (8)
260	720 (11)
240	1070 (18)

case the corresponding relaxation function is a result of powder averaging over all jump directions at a distance r and a subsequent averaging over jump lengths:

$$F(Q,t)=\exp\left[-\left(\frac{t}{\tau}\right)^{\beta_{3D}}\right]$$
$$=\exp\left[-\left(\frac{t}{\tau_0}(1-\exp(-Q^2\langle r^2\rangle/6))\right)^{\beta_{3D}}\right]$$
$$=\exp\left[-\left(\frac{t}{\tau_0}\left(\int_0^\infty P_{3D}(r)dr\left(1-\frac{\sin Qr}{Qr}\right)\right)\right)^{\beta_{3D}}\right], \quad (6)$$

where the spherical Bessel function of zeroth order, $j_0=(1/Qr)\sin(Qr)$, originates from the powder averaging, and

$$P_{3D}(r)=\frac{2r^2}{r_0^3\sqrt{2\pi}}\exp(-r^2/2r_0^2) \quad (7)$$

is the normalized scalar distribution of jump lengths with mean-square jump length $\langle r^2\rangle=3r_0^2$. For a jump diffusion process with a fixed jump length L_0, the relaxation function takes a simpler form:

$$F(Q,t)=\exp\left[-\left(\frac{t}{\tau}\right)^{\beta_{3D}}\right]$$
$$=\exp\left[-\left(\frac{t}{\tau_0}\left(1-\frac{\sin QL_0}{QL_0}\right)\right)^{\beta_{3D}}\right]. \quad (8)$$

While the parameter τ_0 should be independent of the dimensionality of the system, it may seem that the determination on the average residence time using Eq. (4) might be affected if one uses the values of β_{3D} obtained from applying the relaxation function (6) to describe the motion of species confined onto the surface of small crystallites, whose true distribution of residence times may be characterized by a different value, β_{2D}. For such species performing two-dimensional rather than three-dimensional jumps, the powder averaging over all the crystallites has to be carried out,[14,15] and the relaxation function becomes

$$F(Q,t)=\frac{1}{4\pi}\int_0^{2\pi}d\varphi\int_0^{\pi}\sin\theta d\theta\,\exp\left[-\left(\frac{t}{\tau_0}\left(\int_0^\infty P_{2D}(r)\right.\right.\right.$$
$$\left.\left.\left.\times dr(1-J_0(Qr\sin\theta))\right)\right)^{\beta_{2D}}\right], \quad (9)$$

where the cylindrical Bessel function of zeroth order, J_0, replaces the spherical Bessel function in Eq. (6), and

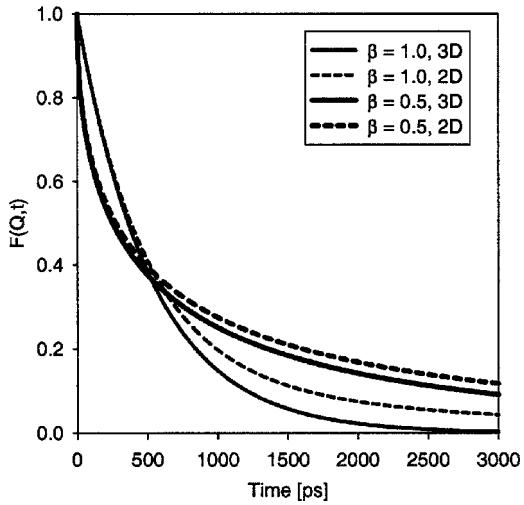

FIG. 6. An illustration of the effect of two dimensionality on the stretched and nonstretched exponential relaxation functions calculated at $Q=1.0$ Å^{-1} for the residence time of 500 ps and the jump length of 3 Å.

$$P_{2D}(r)=\frac{r}{r_0^2}\exp(-r^2/2r_0^2) \quad (10)$$

is the normalized scalar distribution of jump lengths with mean-square jump length $\langle r^2\rangle=2r_0^2$. Again, for a two-dimensional diffusion process with a fixed jump length of L_0, the relaxation function takes a simpler form:

$$F(Q,t)=\frac{1}{4\pi}\int_0^{2\pi}d\varphi\int_0^{\pi}\sin\theta d\theta\exp\left[-\left(\frac{t}{\tau_0}(1\right.\right.$$
$$\left.\left.-J_0(QL_0\sin\theta)\right)^{\beta_{2D}}\right]. \quad (11)$$

For a two-dimensional diffusion process with either a fixed diffusion jump length or a distribution of jump lengths, the relaxation function becomes a superposition of the stretched exponential terms instead of a single stretched exponential term.

Figure 6 illustrates the difference between the stretched and nonstretched relaxation functions calculated at $Q=1.0$ Å^{-1} for arbitrarily chosen parameters $\tau_0=500$ ps and $L_0=3$ Å using Eqs. (8) and (11) for three- and two-dimensional diffusion processes, respectively. As one can see, the two dimensionality and the stretching of an exponential term have completely different effects on the relaxation function. The former yields the relaxation functions that are more slowly decaying at long times (for both stretched and nonstretched exponentials). This effect is analogous to having more peaked scattering functions in the energy space.[7,14,15] Figure 6 demonstrates that the relaxation function for a two-dimensional diffusion process with a particular parameter β, while being somewhat different from the corresponding relaxation function for the three-dimensional process, is also completely different from three- or two-dimensional relaxation functions with a different value of β. In other words, a fit of the two-dimensional diffusion data with the three-dimensional relaxation function should not significantly affect the values of parameter β determined from the fit.

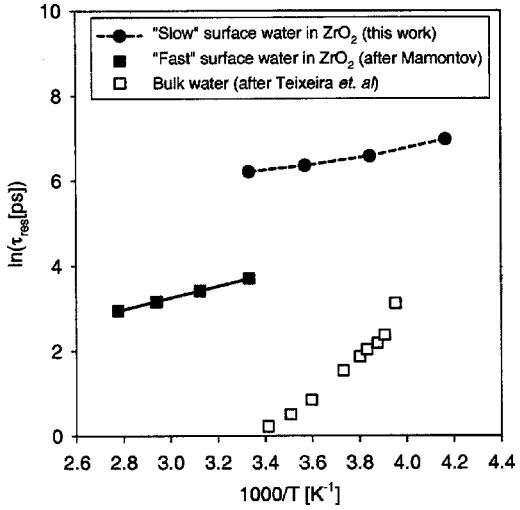

FIG. 7. Comparison of the temperature dependence of residence time for the translational diffusion component of "slow" (this work) and "fast" (after Mamontov, Ref. 7) surface water in ZrO_2 and bulk water (after Teixeira *et al.*, Ref. 16). The error bars for the slow diffusion data are within the filled symbols, and the dashed line is drawn as a guide for the eye.

We have actually verified that using the relaxation function described by Eqs. (9) and (10) instead of that described by Eqs. (6) and (7) to fit the data has virtually no effect on the Q-averaged values of β. Thus, the residence times calculated using Eqs. (4) and (5) should be unaffected even if the diffusion of the "slow" water is quasi-two-dimensional. While we cannot determine the jump distance parameters reliably because of the lack of low-Q data, in principle using the expressions for two- rather than for three-dimensional diffusion process can be expected to have a significant impact on the values of the jump distance.[7] To a smaller extent, using two- instead of three-dimensional relaxation function also affects the apparent fraction of the elastic scattering.

IV. DISCUSSION

Figure 7 shows the temperature dependence of the residence time of the translational diffusion component for surface water in ZrO_2 compared to bulk water. The neutron backscattering experiment described in this work reveals the motion of the slow surface water, whose translational dynamics at room temperature is slower by more than two orders of magnitude compared to bulk water,[16] and by an order or magnitude compared to the "fast" surface water studied in the previous neutron time-of-flight experiment.[7] Interestingly, despite much larger difference in the time scale of dynamics, the temperature dependence for the slow surface water bears more similarity to bulk water than the fast surface water. While the fast surface water shows strictly Arrhenius-type behavior (at least in the studied temperature range of 300–360 K), the slow surface water exhibits a non-Arrhenius temperature dependence similarly to bulk water. Note that the error bars for the slow component in Fig. 7 are within the symbols, and the dashed line is drawn through the data points as a guide for the eye. The residence times longer than one would expect at $T=260$ and 240 K based on the Arrhenius-type temperature dependence are not an artifact caused by insufficient instrument resolution. If the instrument resolution were insufficient to cover the long-time end of the time distribution spectrum, this would result in the measured average residence time being shorter compared to the true average residence time that would be obtained from probing the whole distribution of the residence time spectrum. That is, an instrument resolution insufficient to resolve the very slow motions could only distort the temperature dependence to make the average residence time at lower temperatures appear not longer, but shorter compared to the true average residence time.

The non-Arrhenius temperature dependence of the residence time for the translational diffusion component of the slow surface water as shown in Fig. 7 suggests the presence of a singularity in the dynamics of slow water at temperatures below 240 K, the effect analogous to the structural transition in supercooled bulk[17] and confined water.[18–20] Fitting the temperature dependence of the slow surface water with a power law, $\tau=\tau_0(T/T_s-1)^{-\gamma}$, yields the singularity temperature $T_s=224\pm1$ K. The Vogel–Fulcher–Tamman (VFT) law fitting, $\tau=\tau_0\exp(DT_0/(T-T_0))$, yields the glass transition temperature $T_0=189\pm1$ K. The quality of the fits is demonstrated in Fig. 8. The existence of such a singularity indicates the importance of the cooperative effects in the slow surface water dynamics. Thus, the slow surface water is intrinsically different from the previously studied fast surface water. The molecules of the latter, associated with the outer hydration layer, form less than four hydrogen bonds with the nearest neighbors. As a result, their translational motion can be viewed as a thermally activated, single-particle Arrhenius-type surface jump diffusion process, where cooperative phenomena are not observed. On the other hand, both the non-exponential character of the relaxation function for the slow surface water and its non-Arrhenius translational dynamics strongly suggest that the molecules of this water component are in direct contact with a larger number of neighboring water molecules. It is thus natural to associate the slow surface water with the water molecules of the inner hydration layer. Since some of the bonds formed by these molecules are with immobile water species (hydroxyl groups) in direct contact with the oxide surface, much longer residence times are observed for the translational diffusion component of the inner hydration layer compared to bulk water.

Interestingly, the temperature dependence of the translational diffusion coefficient somewhat similar to our temperature dependence of the translational residence time was observed in hydrated *N*-acetyl-leucine-methylamide.[6] In the concentrated solution of this protein, the dynamics of water associated with the single inner hydration layer was clearly non-Arrhenius, whereas in the less concentrated solution, that is, in the presence of extra hydration layers, the water dynamics was only weakly non-Arrhenius. This similarity is even more interesting in view of the fact that more than 50% of the protein's surface is hydrophobic, while the hydroxylated surface of ZrO_2 is hydrophilic.

As we have discussed in the previous paper,[7] the ZrO_2 sample has about two layers of molecular water on top of the surface hydroxyl groups, and, except for small-angle and Bragg scattering, the signal is dominated by the scattering from hydrogen atoms. With similar areal densities for all the

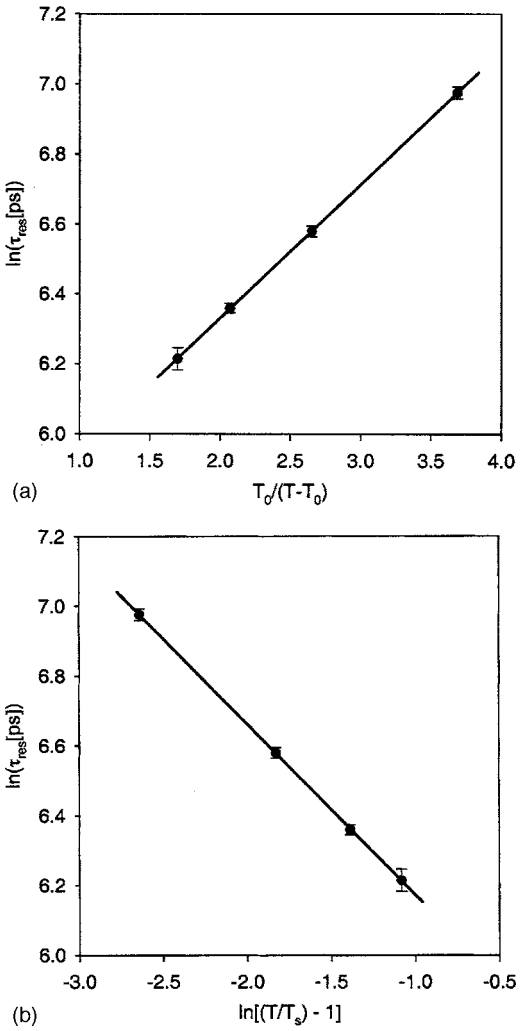

FIG. 8. The temperature dependence of residence time for the translational diffusion component of slow surface water in ZrO_2 (a) fitted with a VFT law, $\tau=\tau_0\exp(DT_0/(T-T_0))$, and plotted as a function of $T_0/(T-T_0)$, $T_0=189$ K (b) fitted with a power law, $\tau=\tau_0(T/T_s-1)^{-\gamma}$, and plotted as a function of $\ln(T/T_s-1)$, $T_s=224$ K.

water layers, the outer and inner hydration layers comprise about 40% of the hydrogen atoms each, and the layer of surface hydroxyl groups accounts for about 20% of the hydrogen atoms. The dynamics of the outer layer is too fast to be seen in the Q range of our backscattering experiment with a limited dynamics range, and only contributes to the background. Thus, if all the water molecules of the inner hydration layer contribute to the quasielastic signal, one would expect to observe the fraction of the elastic scattering [parameter x in Eq. (3)] of about 1/3 due to immobile OH groups. Instead, we found that $x\approx 2/3$ and is temperature independent through the measured temperature range of 240–300 K. This indicates that only a fraction (about one-half) of molecules of the inner hydration layer is mobile on the time scale of the backscattering spectrometer, whereas other molecules of the inner hydration layer contribute to the elastic signal along with the surface hydroxyl groups. It is possible, however, that an experiment with an even higher-energy resolution (such as neutron spin echo) would yield a more stretched relaxation function and a smaller elastic scattering fraction and reveal the motion of those molecules of the inner hydration layer that are too slow to be observed in our backscattering experiment. Another possibility is the presence of water molecules in direct contact with the oxide surface, which are slow and thus contribute to the elastic signal, increasing the measured fraction of the elastic scattering.

The amount of data on the neutron-scattering studies of surface water dynamics available in the literature that can be compared with our results is very limited. Besides our previous work on surface water in ZrO_2,[7] there was a study by Kuroda *et al.*[21] of surface water in Cr_2O_3 in the temperature range of 273–321 K and Takahara *et al.*[22] of surface water in SrF_2 and ZnO in the temperature range of 203–298 K. In these studies, the dynamics of monolayers of water adsorbed either on hydroxylated oxide surfaces or on top of the immobile surface water molecules in the case of SrF_2 was studied using time-of-flight neutron spectrometers with full width at half maximum (FWHM) resolution of 28 and 15 μeV. In all these systems, the residence time of tens of picoseconds was measured for adsorbed water, and an Arrhenius-type temperature dependence of the residence time was observed. These results are analogous to our previous findings on the dynamics of the outer layer of surface water in zirconium oxide,[7] which suggests that time-of-flight neutron spectroscopy with a resolution sufficient to probe the dynamics in the range of tens of picoseconds is sensitive to the translational motion of the topmost hydration layer, the molecules of which participate in a surface jump diffusion process. The dynamics of the monolayer of surface water in ZrO_2 (with removed outer hydration layer) could then be expected to be similar to the dynamics of monolayers of surface water in Cr_2O_3, SrF_2, and ZnO, as well as the dynamics of the outer hydration layer in ZrO_2. On the other hand, the presence of the outer hydration layer probably slows down the dynamics of the inner hydration layer because the molecules of the latter no longer have a reduced number of hydrogen bonds with the neighboring water molecules. Larger number of hydrogen bonds for the molecules of the inner hydration layer makes their translational motion more similar to that in bulk water as indicated by the non-Arrhenius temperature dependence of the residence time. In other words, we propose that the dynamics of the inner hydration layer in the range of hundreds of picoseconds as we studied in the neutron backscattering experiment could be observed only in the presence of the outer hydration layer. Should the outer hydration layer be removed, the molecules of the hydration layer in direct contact with the surface hydroxyl groups would form fewer hydrogen bonds and exhibit a faster dynamics similar to that of the now removed outer hydration layer.

It should be noted that a separation into fast and slow components has been previously observed for interfacial water diffusion in a fully hydrated Na-vermiculite using two neutron spectrometers with different energy resolutions.[13,23] Similarly to our findings, the dynamics of the water molecules that were in contact only with other water molecules was faster by more than an order of magnitude compared to that of the molecules interacting with the surface and/or the intercalated ions.

V. CONCLUSION

A high-resolution QENS study of surface water dynamics in ZrO_2 in the temperature range of 240–300 K has demonstrated the presence of a slow (hundreds of picoseconds) translational diffusion component that appeared as an elastic line in the previous study of the same system with lower resolution. This slow component was ascribed to the translational mobility of the inner hydration layer in the sample having about two layers of molecular water on top of the surface hydroxyl groups. Because some of the bonds formed by these molecules are with immobile water species (surface hydroxyl groups), much longer residence times are observed for the translational diffusion component of the inner hydration layer compared to bulk water. The relaxation function of the motion observed could be described by a stretched exponential indicating a distribution of relaxation times. Unlike the temperature dependence of the residence time previously observed for the outer hydration layer, the one observed for the inner hydration layer was non-Arrhenius, suggesting that the molecules of the inner hydration layer form more hydrogen bonds with the neighboring water molecules. The rearrangement of these molecules is a more complex process than surface diffusion jumps performed by the molecules of the outer hydration layer. We propose that it is the presence of the outer hydration layer that slows down the dynamics of the inner hydration layer to hundreds of picoseconds from tens of picoseconds, which is the characteristic value for the translational dynamics of the topmost hydration layer.

ACKNOWLEDGMENTS

The author is thankful to D. Clough of Magnesium Elektron Inc. for providing the sample and to C. Brown and D. Neumann for critical reading of the manuscript. Utilization of the DAVE package for the data analysis is acknowledged. This work utilized facilities supported in part by the National Science Foundation under Agreement No. DMR-0086210.

[1] J.-M. Zanotti, M.-C. Bellissent-Funel, and S. H. Chen, Phys. Rev. E **59**, 3084 (1999).
[2] H. Paoli, A. Méthivier, H. Jobic, C. Krause, H. Pfeifer, F. Stallmach, and J. Kärger, Microporous Mesoporous Mater. **55**, 147 (2002).
[3] L. P. Aldridge, H. N. Bordallo, and A. Desmedt, Physica B **350**, 565 (2004).
[4] R. E. Lechner, N. A. Dencher, J. Fitter, and G. Büldt, Phys. Scr., T **T45**, 236 (1992).
[5] M.-C. Bellissent-Funel, J.-M. Zanotti, and S. H. Chen, Faraday Discuss. **103**, 281 (1996).
[6] D. Russo, R. K. Murarka, G. Hura, E. Verschell, J. R. D. Copley, and T. Head-Gordon, J. Phys. Chem. B **108**, 19885 (2004).
[7] E. Mamontov, J. Chem. Phys. **121**, 9087 (2004).
[8] A. Meyer, R. M. Dimeo, P. M. Gehring, and D. A. Neumann, Rev. Sci. Instrum. **74**, 2759 (2003).
[9] P. L. Hall and D. K. Ross, Mol. Phys. **42**, 673 (1981).
[10] L. J. Smith, D. L. Price, Z. Chowdhuri, J. W. Brady, and M.-L. Saboungi, J. Chem. Phys. **120**, 3527 (2004).
[11] S. H. Chen, C. Liao, F. Sciortino, P. Gallo, and P. Tartaglia, Phys. Rev. E **59**, 6708 (1999).
[12] F. Mansour, R. M. Dimeo, and H. Peemoeller, Phys. Rev. E **66**, 041307 (2002).
[13] J. Swenson, R. Bergman, and S. Longeville, J. Chem. Phys. **115**, 11299 (2001).
[14] R. Stockmeyer, Ber. Bunsenges. Phys. Chem. **80**, 625 (1976).
[15] A. Renouprez, P. Fouilloux, R. Stockmeyer, H. M. Conrad, and G. Goeltz, Ber. Bunsenges. Phys. Chem. **81**, 429 (1977).
[16] J. Teixeira, M.-C. Bellisent-Funel, S.-H. Chen, and A. J. Dianoux, Phys. Rev. A **31**, 1913 (1985).
[17] R. J. Speedy, and C. A. Angell, J. Chem. Phys. **65**, 851 (1976).
[18] J. Swenson, J. Phys.: Condens. Matter **16**, S5317 (2004).
[19] L. Liu, A. Faraone, C.-Y. Mou, C.-W. Yen, and S.-H. Chen, J. Phys.: Condens. Matter **16**, S5403 (2004).
[20] A. Faraone, L. Liu, C.-Y. Mou, C.-W. Yen, and S.-H. Chen, J. Chem. Phys. **121**, 10843 (2004).
[21] Y. Kuroda, S. Kittaka, S. Takahara, T. Yamaguchi, and M.-C. Bellisent-Funel, J. Phys. Chem. B **103**, 11064 (1999).
[22] S. Takahara, S. Kittaka, T. Mori, Y. Kuroda, T. Yamaguchi, and K. Shibata, J. Phys. Chem. B **106**, 5689 (2002).
[23] J. Swenson, R. Bergman, and W. S. Howells, J. Chem. Phys. **113**, 2873 (2000).